LARGE SCALE STRUCTURE AND COHERENT FINE SCALE EDDIES IN HIGH REYNOLDS NUMBER TURBULENT MIXING LAYERS

Shiki Iwase
Dept. Mechanical and Aerospace Eng., Tokyo Institute of Technology,
2-12-1 Ookayama, Meguro-ku, Tokyo 152-8552, Japan
siwase@mes.titech.ac.jp

Mamoru Tanahashi
Dept. Mechanical and Aerospace Eng., Tokyo Institute of Technology,
2-12-1 Ookayama, Meguro-ku, Tokyo 152-8552, Japan
mtanahas@mes.titech.ac.jp

Toshio Miyauchi
Dept. Mechanical and Aerospace Eng., Tokyo Institute of Technology,
2-12-1 Ookayama, Meguro-ku, Tokyo 152-8552, Japan
tmiyauch@mes.titech.ac.jp

ABSTRACT

Direct numerical simulations of temporally developing turbulent mixing layers are conducted to investigate the large scale structure and the coherent fine scale eddies in high Reynolds number turbulent mixing layers. After the mixing transition, the large scale structure of turbulent mixing layer consists of many fine scale eddies and the number of fine scale eddies inside the large scale structure increases with the increase of Reynolds number. Since the scale of coherent fine scale eddies tends to become small compared with the large scale structure, spatial fluctuation of the energy dissipation rate becomes large for the case of high Reynolds number. In addition, the coherent fine scale eddies do not distribute uniformly inside the large scale structure and form relatively large aggregations in the high Reynolds number case. Large Reynolds stress regions are observed between these aggregations of fine scale eddies. This mechanism of production of the Reynolds stress is very similar to that in turbulent channel flow.

INTRODUCTION

Turbulent mixing layer is commonly observed in various industrial equipments such as combustors where fuel and oxidizer are mixed and react. The understanding of turbulence structure in turbulent mixing layer is quite important. With the transition to turbulence, it has been observed that many fine scale eddies appear in turbulent mixing layer (Moser and Rogers, 1991: Tanahashi and Miyauchi, 1995). These fine scale eddies show tube-like features (Tanahashi et al., 1997a) and their properties such as diameter, azimuthal velocity and strain field acting on them well coincide with the fine scale eddies in homogeneous isotropic turbulence (Jimenez et al., 1993: Tanahashi et al., 2000a). The most expected diameter and maximum azimuthal velocity of the fine scale eddies are 8 times of Kolmogorov microscale (η) and 0.5 times of $u'_{\rm rms}$. The eigen values of the strain field are of the order of $u'_{\rm rms}/\lambda$ at the center of coherent fine scale eddies, where λ is the Taylor microscale. The axis of coherent fine scale eddy tends to be parallel to the eigen vector of intermediate eigen value (Tanahashi et al., 2000a, 2001b). The coherent fine scale eddies also exist in turbulent channel flow and MHD homogeneous turbulence, and their characteristics coincide with that in homogeneous isotropic turbulence and in turbulent mixing layer. The distributions of coherent fine scale eddies are closely related to the anisotropy of turbulent free-shear layers (Tanahashi et al., 2000b) and near-wall turbulence (Tanahashi et al., 1999a). Since turbulent energy is highly dissipated around the coherent fine scale eddies, the coherent fine scale structure plays an important role in intermittent character of turbulent energy

Table 1: DNS data of temporally developing turbulent mixing layers.

$Re_{\omega,0}$	$N_x \times N_y \times N_z$	Re_ω	Re_θ	Re_λ
500	$216 \times 325 \times 144$	4018	1071	74.8
700	$288 \times 433 \times 192$	5911	1522	96.5
900	$324 \times 487 \times 216$	8001	1910	97.6
1100	$360 \times 541 \times 240$	8638	2146	99.7
1300	$384 \times 577 \times 256$	11466	2727	137.5
1500	$432 \times 649 \times 288$	13419	3069	147.2
1900	$480 \times 721 \times 320$	15714	3748	153.9

dissipation (Tanahashi et al., 1997b). In turbulent mixing layers, distinct large scale structures (Brown and Roshko, 1974) and coherent fine scale eddies mentioned above always coexist. As the coherent fine scale eddies dissipate the turbulent energy around them and they are the smallest structure in turbulence, investigations of the relation between large scale structure and coherent fine scale eddies will lead the understanding of the energy cascade mechanism of turbulence. In this study, direct numerical simulations (DNS) of temporally developing turbulent mixing layers with different Reynolds number are conducted to investigate the large scale structure and the coherent fine scale eddies in high Reynolds number turbulent mixing layers.

DNS OF TEMPORALLY DEVELOPING TURBULENT MIXING LAYERS

The DNS of temporally developing turbulent mixing layers with different Reynolds number were conducted by using spectral methods in all directions. The initial mean velocity profile was assumed to be hyperbolic tangent : $u(y) = \tanh(2y)$. Three dimensional random perturbation which has the same turbulent intensity profile with the experimental results and banded white noise $|\boldsymbol{k}| < 21$ was superposed on the mean velocity (Tanahashi et al., 2001b). The boundary condition is periodic in the streamwise and spanwise directions, and free-slip boundary condition was used in the transverse direction. Computational domain was selected to be $4\Lambda \times 6\Lambda \times 8/3\Lambda$ for all Reynolds number cases, where Λ is the most unstable wave length for the initial mean velocity profile. In the spanwise direction, the size of the computational domain is selected due to the 3/2 instability of the two-dimensional roller (Pirrehumbert et al., 1982). In the transverse direction, the size is selected to be large enough to avoid mirror vortex effects caused by the free slip boundary condition (Tanahashi and Miyauchi, 1995). Aliasing errors from nonlinear terms in the governing equations are fully removed by 3/2 rule and time integration is conducted by the low-storage 3rd order Runge-Kutta scheme. The Reynolds number based on the initial vorticity thickness and the mean velocity difference ($Re_{\omega,0}$) and grid points are listed in table 1. Computations were carried out until the occurrence of saturation of the subharmonic mode ($t = 150$) for all cases, and the results at $t = 130$ were analyzed to investigate the coherent fine scale eddies and large scale structure in turbulent mixing layers.

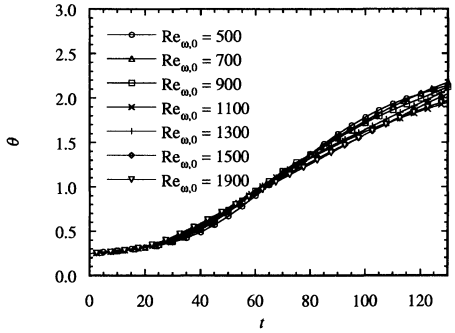

Figure 1: Developments of the momentum thickness.

STATISTICS OF TEMPORALLY DEVELOPING TURBULENT MIXING LAYER

Figure 1 shows the development of momentum thickness for different Reynolds number cases. The momentum thickness is defined by

$$\theta = \frac{1}{(\Delta U)^2} \int_{-L_y/2}^{L_y/2} (U_1 - \overline{u}(y))\,(\overline{u}(y) - U_2)\,dy\ , \tag{1}$$

where U_1 and U_2 represent mean velocity of high and low speed side respectively, and ΔU denotes the mean velocity difference; $U_1 - U_2$. The momentum thickness increases linearly after $t = 30$ and the growth rate does not strongly depend on the Reynolds number.

Developments of Reynolds number based on Taylor microscale (λ) and $\boldsymbol{u}'_{\rm rms}$ at the center of the shear layer, which is denoted by Re_λ, are shown in Fig. 2. The Taylor microscale was calculated from velocity derivatives in the streamwise direction at the center of the shear layer. In contrast with the momentum thickness, Re_λ does not increase linearly with time. Re_λ increases rapidly between $t = 35$ and $t = 65$. After $t = 65$, Re_λ shows plateau with small fluctuation. At $t = 65$, first subharmonic mode shows a peak for all cases, which corresponds to the first pairing of the spanwise rollers in the case of laminar. In these cases, $t = 65$ corresponds to the onset of the transition to turbulence. After the transition,

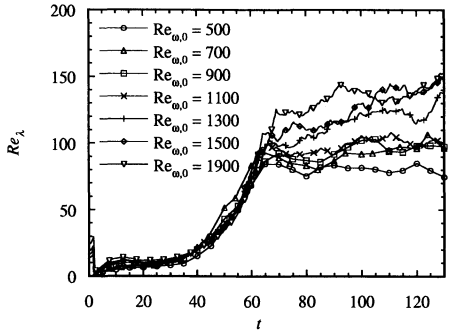

Figure 2: Developments of the Reynolds number based on Taylor microscale and r. m. s. velocity fluctuation

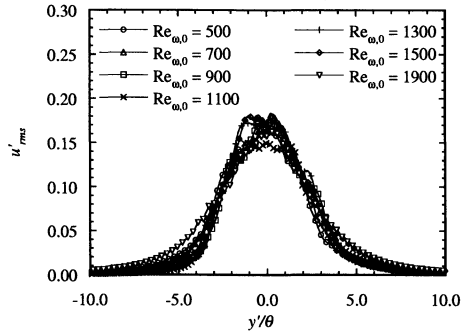

Figure 3: Distributions of r. m. s. streamwise velocity fluctuations at $t = 130$.

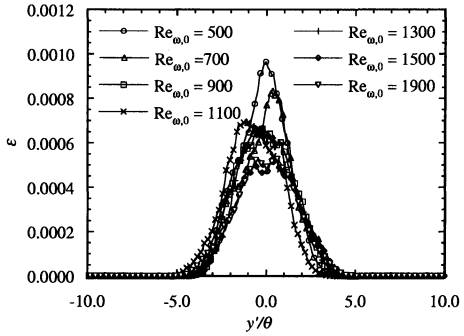

Figure 4: Distributions of the mean energy dissipation rate at $t = 130$.

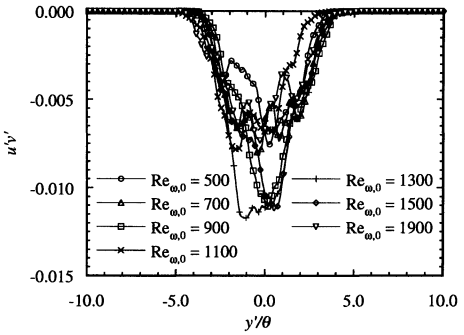

Figure 5: Distributions of the mean Reynolds stress at $t = 130$.

Re_λ does not change so much. Re_ω, Re_θ and Re_λ at $t = 130$ are listed in table 1. Re_θ is the Reynolds number based on the momentum thickness and mean velocity difference.

Distributions of r. m. s. streamwise velocity fluctuation ($u'_{\rm rms}$) and mean energy dissipation rate (ϵ) at $t = 130$ are plotted versus y'/θ in Figs. 3 and 4. The origin of y' was set equal to the position where mean streamwise velocity becomes zero. The profiles of $u'_{\rm rms}$ collapse well and does not depend on the Reynolds number. It is well known that turbulent mixing layer shows a self-similar character at the fully developed state. The profiles of streamwise velocity fluctuations in Fig. 3 reflect this characteristic. In Fig. 4, the energy dissipation rate shows a peak at the center of the shear layer and the peak value of ϵ gradually decreases with the increase of $Re_{\omega,0}$, but the decreasing rate is not constant. At $Re_{\omega,0} = 1300$, the peak value of the energy dissipation rate seems to attain an asymptotic value ($\epsilon \approx 0.006$). However, it decreases again for $Re_{\omega,0} > 1500$. Figure 5 shows profiles of the mean Reynolds stress. The mean Reynolds stress shows a minimal at the center of the shear layer and there is no apparent relation between the minimal value and $Re_{\omega,0}$.

LARGE SCALE STRUCTURE AND COHERENT FINE SCALE EDDIES

Figures 6 and 7 show contour surfaces of second invariant of the velocity gradient tensor for the cases of $Re_{\omega,0} = 700$ and 1900. The second invariant of the velocity gradient tensor is defined by

$$Q = -\frac{1}{2}\left(S_{ij}S_{ij} - W_{ij}W_{ij}\right) , \qquad (2)$$

where S_{ij} and W_{ij} is symmetric and asymmetric part of the velocity gradient tensor. In Figs. 6 and 7, the second invariant is normalized by Kolmogorov microscale and $\boldsymbol{u}'_{\rm rms}$ at the center of the shear layer (Tanahashi et al., 1997b: Tanahashi and Miyauchi, 2001a). Hereafter, all asterisked values are normalized by Kolmogorov microscale and $\boldsymbol{u}'_{\rm rms}$ at the center of the shear layer.

As shown in previous works (Moser and Rogers, 1991, 1993: Tanahashi and Miyauchi, 1995), the transition to turbulence of a mixing layer occurs after the first pairing or before the second pairing of Kelvin-Helmholtz rollers. Once the mixing transition occurred, huge number of coherent fine scale eddies appear for all Reynolds number cases, while the diameter of coherent fine scale eddies obviously decreases with the increase of $Re_{\omega,0}$. It has been shown that the diameter of them is about 8η and the maximum azimuthal velocity is 0.5 $\boldsymbol{u}'_{\rm rms}$ for all cases by using the eddy identification scheme developed in our previous studies

Top View

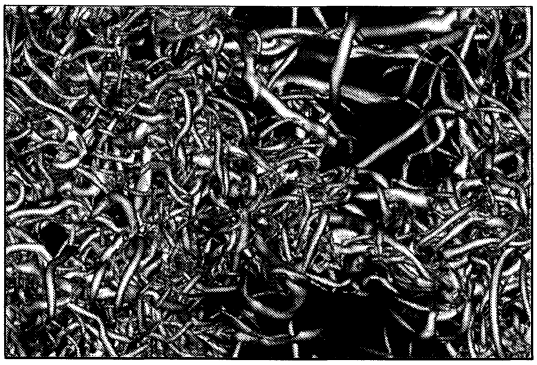

Side View

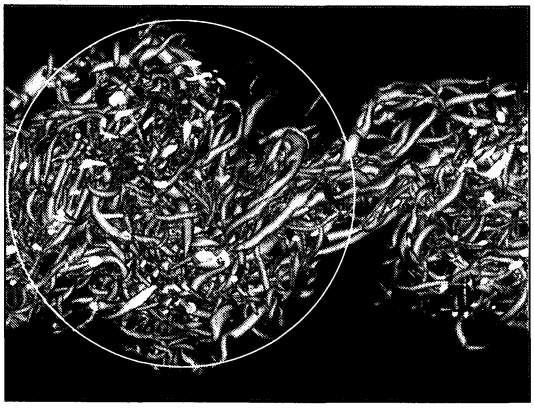

Figure 6: Isosurfaces of the second invariant at $t = 130$ ($Re_{\omega,0} = 700, Q^* \geq 0.01$).

Top View

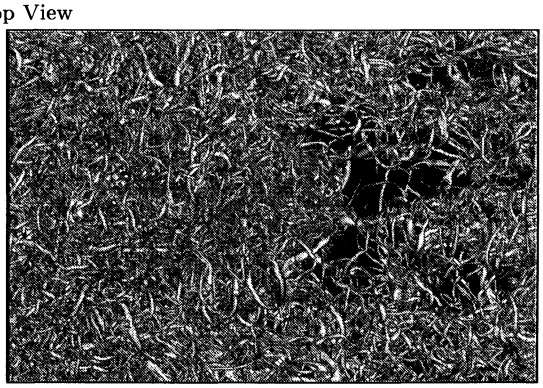

Side View

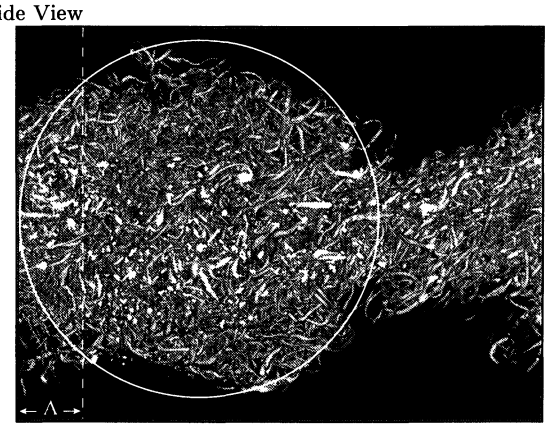

Figure 7: Isosurfaces of the second invariant at $t = 130$ ($Re_{\omega,0} = 1900, Q^* \geq 0.01$).

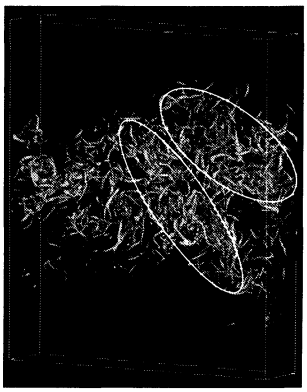

Figure 8: Aggregations of the fine scale eddies at $t = 130$ ($Re_{\omega,0} = 1900, Q^* \geq 0.02$).

(Tanahashi et al., 1997a, 2000a).

The tube-like structures elongated in the streamwise direction in the 'Top View' of Fig. 6 are well-known rib vortices in the braid region. The rib vortices can be identified clearly for low Reynolds number cases, whereas, it is difficult to distinguish the rib vortices in high Reynolds number case. The large scale coherent structures, which have been identified by Brown and Roshko (1974), can also be observed in the present DNS. The circles in the 'Side View' of Figs. 6 and 7 denote so-called large scale coherent structures in the turbulent mixing layers. The number of coherent fine scale eddies which compose the large scale structures increases with the increase of $Re_{\omega,0}$, because scale separation between large scale structures and coherent fine scale eddies becomes large. Figure 8 shows the isosurfaces of the second invariant inside the large scale coherent structure for the case of $Re_{\omega,0} = 1900$. The visualized domain was denoted by 'A' in Fig. 7 and the threshold of the second invariant was selected to 0.02. By choosing this threshold, only the relatively intense coherent fine scale eddies are visualized. The intense coherent fine scale eddies inside the large scale structure do not distribute uniformly and form relatively large aggregations for high Reynolds number case as shown by the circles in Fig. 8. These aggregations of the coherent fine scale eddies are also observed in high Reynolds number homogeneous isotropic turbulence and turbulent channel flow (Tanahashi et al., 2001c).

Since the turbulent energy is highly dissipated around the coherent fine scale eddies (Tanahashi et al., 2000a), the distribution of the turbulent energy dissipation rate will be characterized by the distribution of the coherent fine scale eddies. Figures 9 and 10 show the isosurfaces of the energy dissipation rate (ϵ) with isosurfaces of the second invariant for $Re_{\omega,0} = 700$ and 1900. The threshold was selected to be $\epsilon = 2\epsilon_m$ for the energy dissipation

Top View

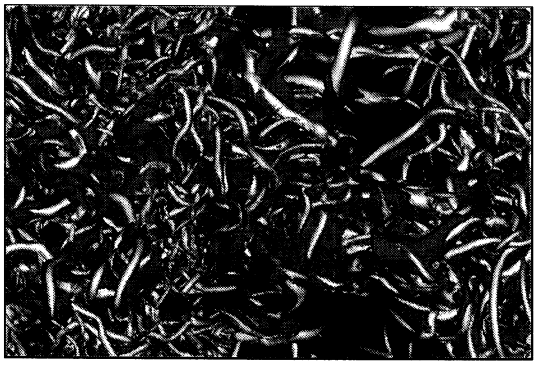

Side View

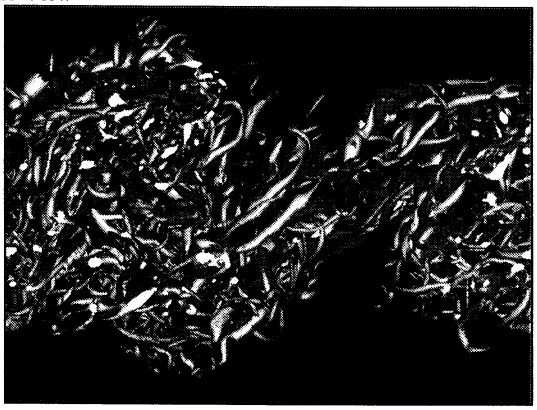

Figure 9: Isosurfaces of the second invariant (white) and energy dissipation rate (gray) at $t = 130$ ($Re_{\omega,0} = 700, Q^* \geq 0.01, \epsilon \geq 2\epsilon_m$).

Top View

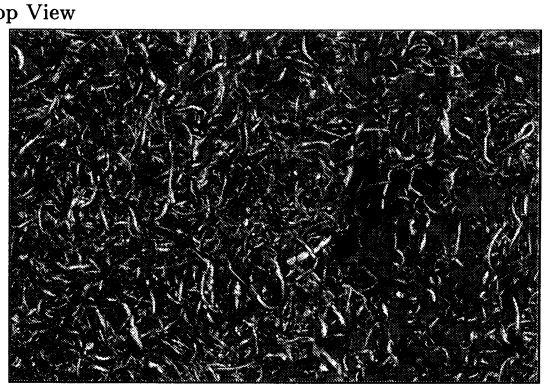

Side View

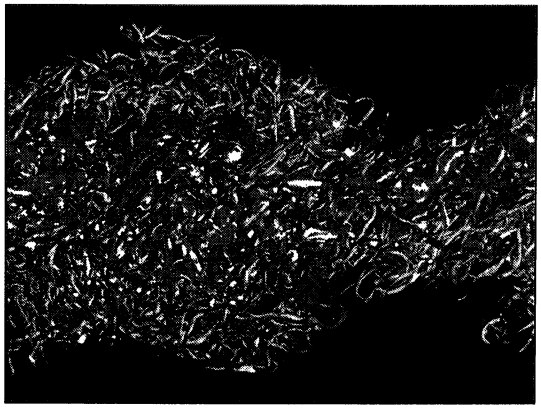

Figure 10: Isosurfaces of the second invariant (white) and energy dissipation rate (gray) at $t = 130$ ($Re_{\omega,0} = 1900, Q^* \geq 0.01, \epsilon \geq 2\epsilon_m$).

rate, where ϵ_m denotes the mean energy dissipation rate at the center of the shear layer. In the case of the highest Reynolds number, the spatial fluctuation of the energy dissipation rate is large, because the scale of coherent fine scale eddies tend to be small compared with the large scale structure for high $Re_{\omega,0}$ as described above.

In general, the mechanism of production of the instantaneous Reynolds stress in turbulent mixing layer is described based on the large scale structure of the mixing layer. Figure 11 shows the isosurfaces of second invariant and instantaneous Reynolds stress for the case of $Re_{\omega,0} = 1900$. The threshold for the instantaneous Reynolds stress is $-u^*v^* > 2.0$. Similar to the energy dissipation rate, spatial fluctuation of the instantaneous Reynolds stress becomes large with the increase of the $Re_{\omega,0}$. Figure 12 shows relationship between the instantaneous Reynolds stress and the coherent fine scale eddies inside the large scale structures. To make clear the relationship more apparent, only the isosurfaces of second invariant with threshold = 0.01 is shown. Visualized regions for both figures is the same in Fig. 8. The region with large instantaneous Reynolds stress can be observed between the aggregations of the coherent fine scale eddies. The distribution of the instantaneous Reynolds stress can not be explained by the large scale structure in the mixing layer. In the conventional interpretation, it has been considered that elliptic large scale coherent structure make the Reynolds stress negative. The relationship between instantaneous Reynolds stress and coherent fine scale eddies is also observed in other kind of turbulent flow. In the case of high Reynolds number turbulent channel flows, large instantaneous Reynolds stress regions are observed between the coherent fine scale eddies (Tanahashi et al., 1999b).

CONCLUSIONS

In this study, DNS of temporally developing turbulent mixing layers are conducted to investigate the large scale structure and the coherent fine scale eddies in high Reynolds number turbulent mixing layer.

The large scale structure of the turbulent mixing layer consists of many coherent fine scale eddies after the transition to turbulence and number of the coherent fine scale eddies inside the large scale structure increases with the increase of $Re_{\omega,0}$. Since the scale of coherent fine scale eddies tend to become

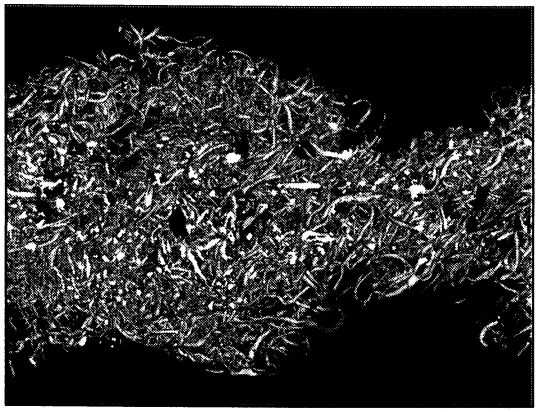

Figure 11: Isosurfaces of the second invariant (white) and Reynolds stress (gray) at $t = 130$ ($Re_{\omega,0} = 1900, Q^* \geq 0.01, -u^*v^* \geq 2$).

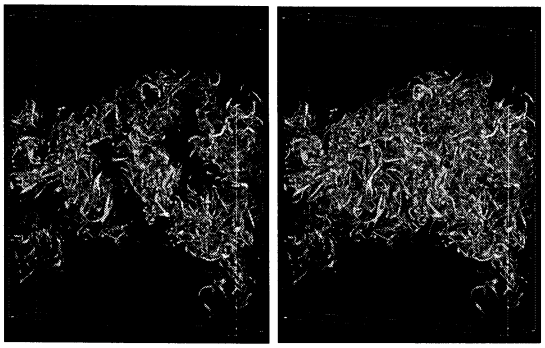

Figure 12: Relation between the coherent fine scale eddies and Reynolds stress (gray) at $t = 130$ ($Re_{\omega,0} = 1900$). Left : isosurfaces of the second invariant ($Q^* \geq 0.01$) and instantaneous Reynolds stress ($-u^*v^* \geq 2$), right : isosurfaces of the second invariant ($Q^* \geq 0.01$).

small compared with the large scale structure, spatial fluctuations of the energy dissipation rate becomes large for high Reynolds number case. The coherent fine scale eddies inside the large scale structure make aggregations with medium scale for high Reynolds number case and relatively large instantaneous Reynolds stress are observed between these aggregations. This mechanism of production of the Reynolds stress can not be explained by the conventional interpretation based on the large scale coherent structure in turbulent mixing layer.

ACKNOWLEGEMENT

This work has been partially supported by Grant-in-Aid for Science Research on Priority Areas (B) from the Ministry of Education, Culture, Sports, Science and Technology of Japan.

REFERENCE

Brwon, G. L. and Roshko, A., 1974, "On density effects and large structure in turbulent mixing layers", *J. Fluid Mech*, 64, 775.

Jimenez, J., Wray, A. A., Saffman, P. G. and Rogallo, R. S., 1993, "The structure of intense vorticity in isotropic turbulence", *J. Fluid Mech.* 255, 65.

Moser, R. D. and Rogers, M. M., 1991, "Mixing transition and the cascade to small scales in a plane mixing layer", *Phys. Fluids*, A3, 1128.

Moser, R. D. and Rogers, M. M., 1993, "The three-dimensional evolution of a plane mixing layer: paring and transition to turbulence", *J. Fluid Mech.*, 247, 275.

Pirrehumbert, R. T. and Windnall, S. E., 1982, "The two- and three- dimensional instabilities of a spatially periodic shear layer", *J. Fluid Mech.*, 114, 327.

Tanahashi, M. and Miyauchi, T., 1995, "Small scale eddies in turbulent mixing layer", *Proc. 10th Symposium on Turbulent Shear Flows*, 79.

Tanahashi, M., Miyauchi, T. and Matsuoka, K., 1997a, "Coherent fine scale structures in temporally developing turbulent mixing layers", *Turbulence, Heat and Mass Transfer 2*, Delft University Press, 461.

Tanahashi, M., Miyauchi, T. and Ikeda, J., 1997b, "Scaling low of coherent fine scale structure in homogeneous isotropic turbulence", *Proc. 11th Symp. Turbulent Shear Flows*, Vol.1, 4-17.

Tanahashi, M., Das, S. K., Shoji, K. and Miyauchi, T., 1999a, "Coherent fine scale structure in turbulent channel flows", *Trans. JSME*, 65B, 638.

Tanahashi, M., Shiokawa, S. and Miyauchi, T., 1999b, "Reynolds number dependence of turbulence structure in near-wall turbulence", *Proc. 31st Symp. Turbulence in Japan*, 267.

Tanahashi, M., Iwase, S. and Miyauchi, T., 2000a, "Appearance and alignment with strain rate of coherent fine scale eddies in turbulent mixing layer", *Proc. the 8th European Turbulence Conference. Advances in Turbulence VIII*, 655.

Tanahashi, M., Miyauchi, T., and Matsuoka, K., 2000b, "Statistics of coherent fine scale structure in turbulent mixing layers", *Developments in Geophysical Turbulence*, Kluwer academic publishers, 205.

Tanahashi, M. and Miyauchi, T., 2001a, "Coherent fine scale eddies in turbulent shear flows and it's relation to anisotropy", *Geometry and Statistics of Turbulence*, Kluwer Academic Publishers, 77.

Tanahashi, M., Iwase, S. and Miyauchi, T., 2001b, "Appearance and alignment with strain rate of coherent fine scale eddies in turbulent mixing layer", *Journal of Turbulence*, to be published.

Tanahashi, M., Iwase, S., Shiokawa, S., Yanagawa, T. and Miyauchi, T., 2001c, "Reynolds number dependence of the coherent fine scale eddies in turbulence", *Proc. 16th Symp. Numerical Simulation of Turbulence in Japan*, 14.